Short Communication

Journal of Physical Organic Chemistry

Received: 10 August 2013, Revised: 12 December 2013, Accepted: 05 January 2014, Published online in Wiley Online Library: 31 January 2014

(wileyonlinelibrary.com) DOI: 10.1002/poc.3288

Electrochemical reduction of 3-phenyl-1, 2-benzisoxazole 2-oxide on boron-doped diamond†

Martin Kociolek[a]*, Jason Bennett[a] and Jerry Casbohm[a]

The bioreduction of *N*-oxide compounds is the basis for the mode of action of a number of biologically active molecules. These compounds are thought to act by forming a reactive oxygen species through an intracellular reduction and subsequent redox cycling process within the organism. With these results in mind, the preliminary investigation into the electrochemical reduction of the benzisoxazole 2-oxide ring system was undertaken, with the thought that this class of compounds would reduce in a similar fashion to other *N*-oxide heterocycles. The electrochemical reduction of 3-phenyl-1,2-benzisoxazole 2-oxide on boron-doped diamond was studied using cyclic and square wave voltammetry as well as controlled potential electrolysis and HPLC for qualitative identification of the reaction products. It was found that the reduction proceeded with an initial quasi-reversible one-electron reduction followed by the very fast cleavage of either the endocyclic or exocyclic N–O bond. Subsequent electron transfer and protonation resulted in an overall two-electron reduction and formation of the 2-hydroxyaryl oxime and benzisoxazole. These results are analogous to those observed in the electrochemical reduction of other heterocyclic *N*-oxides albeit the reduction of the benzisoxazole *N*-oxides takes place at a more negative potential. However, these encouraging results warrant further investigation into the reduction potential of substituted benzisoxazole *N*-oxides as well as to elucidate and characterize the nature of the intermediate species involved. Copyright © 2014 John Wiley & Sons, Ltd.

Keywords: *N*-oxides; electrochemical reduction; boron-doped diamond; cyclic voltammetry; square wave voltammetry

INTRODUCTION

The bioreduction of *N*-oxide compounds is the basis for the mode of action of a number of biologically active molecules. These compounds are thought to act by forming a reactive oxygen species through an intracellular reduction and subsequent redox cycling process within the organism. This is the basis for the anti-infective activity exhibited by a number of different classes of *N*-oxide compounds including quinoxaline 1,4-di-*N*-oxides[1] (anti-infectious), benzofuroxans[2,3] (antiprotozoal) and indolone-*N*-oxides[4] (antimicrobial). While the mode of action of these compounds has been proposed, the exact mechanism by which these drugs act in biological systems has not been fully elucidated. In order to shed light on how these systems behave, a more detailed investigation of the possible reaction mechanism is warranted. For this reason, the electrochemical reduction of a number of these compounds has been investigated. The reduction of benzofuroxans has been proposed to proceed via a two-step reduction mechanism, first forming a radical species and subsequently reducing to result in either ring opening of the furoxan or deoxygenation of the ring.[2] Isoxazoles and related compounds have also been shown to undergo electrochemical ring opening.[5] In a similar manner, oximes have been shown to reduce by way of a facile N–O bond cleavage.[6] With these results in mind, the preliminary investigation into the electrochemical reduction of the benzisoxazole 2-oxide ring system by cyclic voltammetry, square wave voltammetry (SWV) and constant potential electrolysis was undertaken, with the thought that this class of compounds would reduce in a similar fashion to other *N*-oxide heterocycles. Boron-doped microcrystalline diamond (BDD) electrodes were chosen due to their known anti-fouling properties and wide potential window.

RESULTS

Initial investigation involved cyclic voltammetry of a 3 mM solution of 3-phenyl-1,2-benzisoxazole 2-oxide (**1a**) dissolved in 0.1 M tetrabutylammonium tetrafluoroborate and acetonitrile (TBATFB/ACN) at a BDD electrode. Figure 1 shows a representative cyclic voltammogram (CV). The potential was scanned positive from −1.0 V to 1.0 V, then negative to −3.0 V at a rate of 0.5 V/s. The voltammogram exhibits no distinguishable features during the initial forward scan. Scanning in the negative direction shows a reduction at approximately −2.6 V (**I**), which can be attributed to the reduction of the *N*-oxide. Upon scanning forward, an oxidation is observed at −0.15 V (**II**). Due to the large peak separation, it seems unlikely that **II** is due to the reoxidation of the *N*-oxide radical anion. To examine this relationship closer, SWV was performed, the results of which are shown in the Fig. 1 inset. The

* *Correspondence to: Martin Kociolek, Penn State Erie, The Behrend College, School of Science, Erie, USA.*
E-mail: mgk5@psu.edu

a *M. Kociolek, J. Bennett, J. Casbohm*
Penn State Erie, The Behrend College, School of Science, Erie, USA

Copyright © 2014 John Wiley & Sons, Ltd.

Journal of Physical Organic Chemistry

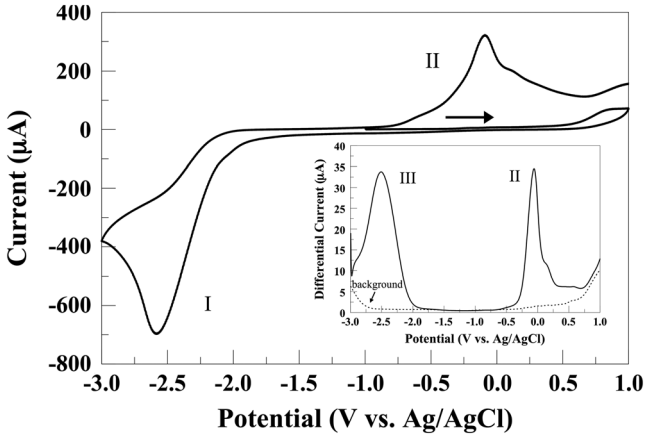

Figure 1. Cyclic voltammogram for 3 mM 1a in 0.1 M TBATFB/ACN at a scan rate of 0.5 V/s. Inset is a square wave voltammogram for the same solution

potential was stepped from −3.0 V (to ensure reduction of the *N*-oxide) to 1.0 V at 5 mV increments, 25 mV amplitude and 15 Hz frequency. The SWV exhibits two oxidation peaks, one similar to the CV at approximately −0.10 V (**II**) and an additional peak at −2.5 V (**III**). Peak **III** likely corresponds to the reoxidation of the radical anion of **1a**, which supports that **II** originates from the oxidation of a different radical anion species. These results are consistent with the electrochemical reduction (E step) of **1a** being followed by a fast chemical (C) step (and hence not being available for reoxidation back to **1a**), referred to as an EC mechanism.

To further investigate the electrochemical behavior of the compounds, CVs were obtained at various scan rates as shown in Fig. 2. Note that the magnitude of the *N*-oxide reduction (**I**) increases linearly with the square root of scan rate, illustrated in Fig. 3, which denotes a diffusion-limited process. According to Savéant[7] the peak current (i_p in A) for an EC reduction mechanism would be expected to increase linearly with the square root of the scan rate ($v^{1/2}$) as shown in Eqn (1):

$$|i_p| = \frac{0.496nF^{3/2}AC^{\circ}D^{1/2}v^{1/2}}{R^{1/2}T^{1/2}} \quad (1)$$

where n is the number of electrons transferred, F is Faraday's constant, A is the electrode area (cm^2), C^o is the bulk concentration of 1a (mol/cm^3), D is the diffusion coefficient of 1a (cm^2/s), R is the gas constant and T is the temperature (K). Since $|i_p/v^{1/2}|$ is the slope

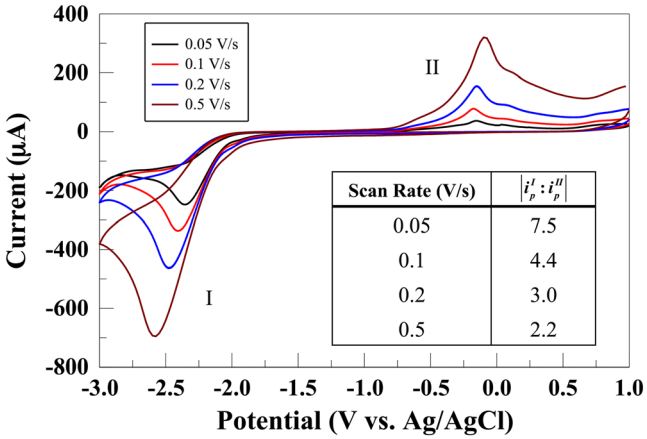

Figure 2. Cyclic voltammogram for 3 mM **1a** in 0.1 M TBATFB/ACN at various scan rates

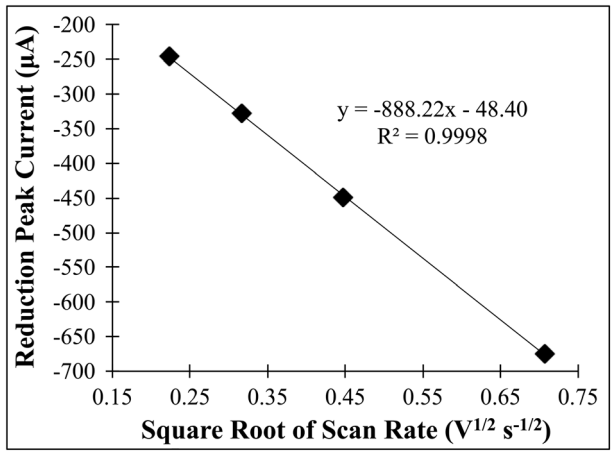

Figure 3. Plot showing the linearity of the peak I current from voltammograms in Fig. 2 with the square root of the scan rate

from Fig. 3 (adjusted to A/(V$^{1/2}$ s$^{-1/2}$)), the number of electrons transferred can be calculated through a simple rearrangement as shown in Eqn (2).

$$n = \frac{|\text{slope}|^{*}R^{1/2}T^{1/2}}{0.496F^{3/2}AC^{\circ}D^{1/2}} \quad (2)$$

Using the slope from Fig. 3, a T of 295 K, an electrode area of 0.2190 cm^2, a bulk concentration of 3×10^{-6} mol/cm^3 and an estimated diffusion coefficient of 2×10^{-5} cm^2/s[8] resulted in a calculated one-electron transfer ($n = 1.01$). This was further supported via potential step chronoamperometry by stepping the potential from 0 V to −3 V and using the well-known Cottrell equation ($n = 0.77$). In addition, preliminary kinetic parameters were calculated and are detailed in the supporting information.

It should be noted that the $i_p^{I} : i_p^{II}$ ratio in Fig. 2 varies with scan rate as indicated in the inset table. The observation that the current of II decreases (to a greater extent relative to I) with decreasing scan rate further supports an EC mechanism. This will be discussed further in the discussion section. The degree of reversibility (R_{DPS}) for the initial electrochemical reduction of **1a** can be approximated using double potential step chronoamperometry by following the initial reduction step (0 V to −3 V for a given time t_R) with an anodic step (−3 V to 0 V for the same amount of time). The R_{DPS} can then be calculated using Eqn ((3)) where $i_c(t_R)$ is the current measured at the end of the initial reduction step and $i_a(2t_R)$ is the current measured in the anodic step after the same amount of time.[7]

$$R_{DPS} = \frac{-i_a(2t_R)/i_c(t_R)}{1 - 1/\sqrt{2}} \quad (3)$$

A system is considered more reversible as the R_{DPS} value approaches 1. The double potential step chronoamperometric experiment (not shown) yielded a $-i_a(2t_R)/i_c(t_R)$ ratio of 0.07366, which resulted in a calculated R_{DPS} value of 0.25. This quasi-reversibility explains why the re-oxidation of **1a** is only visible on the SWV (**III** in Fig. 1 inset) and not on any of the CVs.

The effect of increasing water concentration was investigated by examining both CV and SWV in various ACN/H_2O ratios. These are shown in Fig. 4 and its inset, respectively. There are two significant results from this study. First, the oxidation **II** potential (CV) shifts anodically with increasing water concentration, confirming the

 Copyright © 2014 John Wiley & Sons, Ltd.

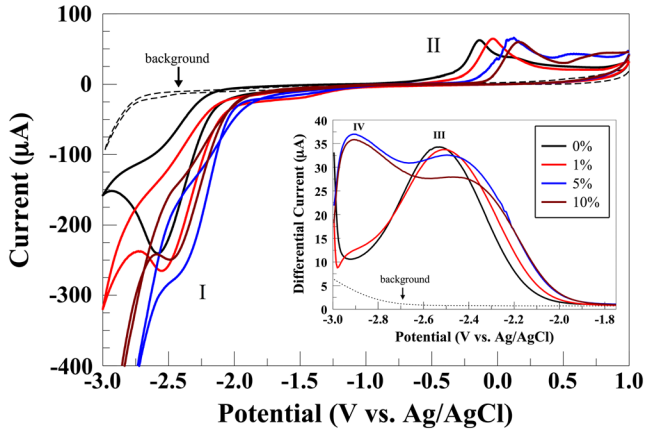

Figure 4. Cyclic voltammogram for 3 mM **1a** in 0.1 M TBATFB/ACN as a function of water content. Inset is the square wave voltammograms for the same solutions

participation of H^+ in the reaction. Comparatively, only a minimal change was observed in the reduction **I** potential in the CV as well as in its corresponding reoxidation **III** in the SWV. The second important result from this study is the emergence of a second oxidation peak (**IV**) at a slightly more negative potential (−2.9 V) than peak **III** at 5 and 10% water concentration.

In order to identify the species produced by the reduction, a qualitative analysis using controlled potential electrolysis was carried out in a custom thin-layer cell using a BDD working electrode. The cell was filled with a 1.0 mM solution of **1a** in 0.1 M TBATBF/ACN and the potential held at −3 V for 1500 s, after which the cell was flushed and the mixture analyzed by HPLC with a PDA detector. In addition to unreacted *N*-oxide, the chromatogram revealed two peaks whose retention times and UV spectra were identical to authentic samples of oxime **3** and benzisoxazole **4**. It should be noted that increasing electrolysis times resulted in a darkening of the reaction mixture, some deposition and peaks early in the chromatogram that were attributed to butylamine from the breakdown of the TBATFB. It is important to note that a two-electron reduction is required to convert the original compound to either of these products; however, the exact nature of the second reduction cannot be elucidated from these results.

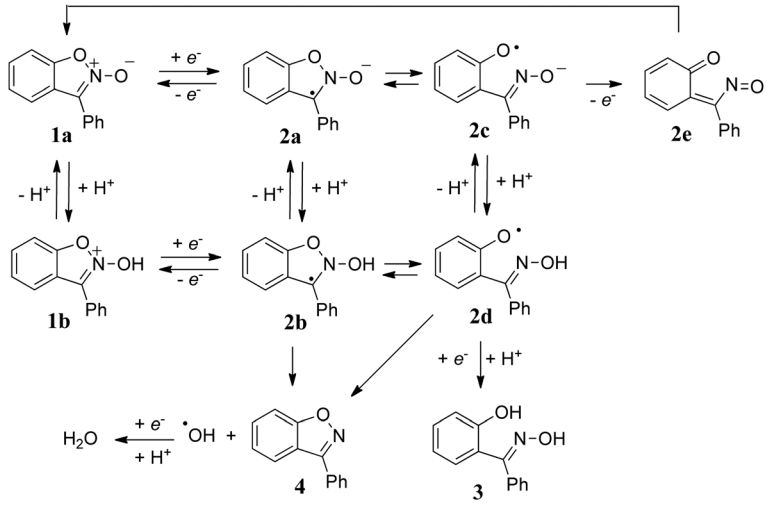

Scheme 1. Proposed mechanism for reduction of *N*-oxide **1a**

DISCUSSION

Given these results and what has been previously reported for the electrochemical reduction of similar heterocyclic *N*-oxides, the reduction mechanism shown in Scheme 1 can be proposed. The initial reduction **I** can be attributed to the one-electron reduction of *N*-oxide **1a** to give radical anion **2a**. Although the reverse oxidation was not observed in the CV, SWV yielded an oxidation peak (**III**) that can be attributed to the oxidation of **2a** to **1a**.

Further analysis of this reaction in aqueous acetonitrile solutions was undertaken, so the effect of either protonation or hydrogen bonding on different species could be observed by changes in the potential for the corresponding waves. Reduction **I** in the CV showed only small changes in potential as the percentage of water was increased. This is consistent with the fact that the equilibrium between neutral **1a** and its protonated form **1b** would likely not change much with the addition of water. The small changes observed would likely be from a small degree of H-bonding to **1a**. In contrast, the SWV showed significant changes with an additional oxidation peak appearing at approximately −2.9 V. These observations can be rationalized by a shifting of equilibrium between **2a** and **2b**, due to protonation of the radical anion. Also likely is that the electron-rich species **2a** possesses a greater degree of H-bonding. Both these factors could explain the presence of two oxidation peaks (**III** and **IV**) in the SWV at higher water content.

Oxidation **II**, observed in the voltammograms, only appears on the return scan after going to −3.0 V. The large difference in potential along with the SWV results suggests that this oxidation is not the reverse of reduction **I** but is consistent with the initial electron transfer being followed by a very fast chemical step resulting in a new species which is then oxidized. In addition, an analysis of the CV at different scan rates was performed. While the magnitudes of peaks I and II both decrease with decreasing scan rate as expected, oxidation II decreased to a greater extent (as given by the ratio of $i_p^{I} : i_p^{II}$). This would be consistent with an EC mechanism. At slower scan rates, the product of the chemical reaction is likely diffusing away from the surface and undergoing further reaction before it could be oxidized; however, higher scan rates allow for reoxidation before further reaction. One hypothesis is that the odd electron species **2a** is undergoing a very fast endocyclic N–O bond cleavage to give the ring-opened species **2c**. A similar process has been reported for oximes, which upon electrochemical reduction, form the radical anion that quickly cleaves to form hydroxide ion and an imine radical.[6] The rate of the N–O bond cleavage in oximes is fast enough that the oxidation wave for the initial radical anion is not observed. In this case, it is also reasonable to believe that the chemical step would be faster than subsequent electron transfer on BDD, which is known to possess semi-metal characteristics.[9] Subsequent reduction of **2c** (or a similar ring-opened species) could result in formation of oxime **3**, which was observed as a product of the controlled potential electrolysis. The exact nature of the species being oxidized (Peak II) and its resulting product are still under investigation; however, it has been previously reported that 2-hydroxyaryl oximes analogous to **3** have been

Copyright © 2014 John Wiley & Sons, Ltd.

electrochemically oxidized to give benzisoxazole *N*-oxides **1a**,[10] making it conceivable that the species being oxidized could be **2c, 2d** or a related species.

Previously reported in the literature, the ortho quinone methide **2e** intermediate has been proposed in the chemical oxidation of oxime **3** to benzisoxazole *N*-oxide **1a**.[10] A mechanism involving the oxidation of **2c** to **2e** and subsequent cyclization to regenerate **1a** would be consistent with our observed results. Modeling of the proposed square scheme involving **1a**, **2a**, **2c** and **2e** yielded a CV consistent with the experimental results, supporting a one-electron reduction (see supporting information).

Analysis of the products of controlled potential electrolysis also showed the presence of benzisoxazole **4**. Formation of this product can be rationalized, by protonation of initial radical anion **2a** to **2b**, which can undergo a fast exocyclic N–O bond cleavage, analogous to oximes, giving benzisoxazole **4** and hydroxyl radical. An alternate pathway to **4** could involve recyclization and loss of hydroxyl radical from **2d**.

The formation of **3** and **4** from *N*-oxide **1a** must require an overall two-electron reduction. Because the CV revealed only a single one-electron reduction, it cannot be unequivocally concluded that these products are being formed on the fast time scale of the CV experiment. However, the observation of a one-electron transfer would not be contradictory to a possible secondary solution-electron transfer mechanism,[11] in which case the second electron could be coming from the oxidation of another single electron species in solution. In the case of the controlled potential electrolysis, the much longer reaction times and smaller solution volume (limiting diffusion) make it more likely that the secondary reduction is happening at the electrode surface, resulting in formation of **3** and **4**.

CONCLUSION

The results of the electrochemical analysis of 3-phenyl-1,2-benzisoxazole 2-oxide (**1a**) using a combination of cyclic and SWV showed a quasi-reversible one-electron reduction followed by a very fast chemical step involving cleavage of either the exocyclic or endocyclic N–O bonds. Subsequent electron transfer and protonation resulted in an overall two-electron reduction and formation of oxime **3** and benzisoxazole **4**. These results are analogous to those observed in the electrochemical reduction of other heterocyclic *N*-oxides albeit the reduction of the benzisoxazole *N*-oxides takes place at a more negative potential. This could in part be a function of the BDD electrode and not just that of the substrate. However, these encouraging results warrant further investigation into the reduction potential of substituted benzisoxazole *N*-oxides as well as to elucidate and characterize the nature of the intermediate species involved.

EXPERIMENTAL

Preparation of 3-phenyl 1,2-benzisoxaozle 2-oxide (1a)

Compound **1a** was prepared as previously reported in the literature, starting with 2-hydroxy benzophenone.[12]

Electrochemical measurements

All electrochemical measurements were performed at room temperature using a single-compartment glass cell and a CH Instruments model 842C Series Electrochemical Analyzer (CH Instruments, Austin, TX). The design of the electrochemical cell was reported previously.[13] BDD electrodes were obtained from Greg Swain at Michigan State University and were grown using a CH_4/H_2 ratio of 0.5%. Details of the electrode growing conditions have been reported previously.[14,15] The diamond working electrode was pressed against the bottom of the glass cell and a Chemraz® O-ring (Ace Glass, Inc.) was used to contain the solution and define the exposed electrode area, 0.22 cm^2. A non-aqueous Ag/AgCl reference electrode (0.01 M $AgNO_3$ + 0.1 M tetrabutylammonium perchlorate in acetonitrile; CH Instruments) was positioned in close proximity to the working electrode using a cracked-glass capillary filled with electrolyte solution. All potentials reported herein are referenced to this electrode. Either a large-area carbon rod or a Pt wire served as the auxiliary electrode. Electrical connection was made to the working electrode by rubbing a graphite rod on the back side of the cleaned Si substrate prior to contacting with a clean Cu plate. Compound **1a** was dissolved in 0.1 M tetrabutylammonium tetrafluoroborate (TBATFB; Alfa Aesar) in acetonitrile (ACN), to yield a final analyte concentration of 3.0 mM. The TBATFB and ACN were reagent grade or better and used without additional purification. The proton study was performed using TBATFB that was dried at room temperature under vacuum and a fresh bottle of extra dry acetonitrile 99.9% stored over molecular sieves and acrosealed® (Acros Organics).

Thin-layer electrolysis measurements

The products of the electrochemical reduction were isolated using controlled potential electrolysis at a BDD electrode in a custom thin-layer flow cell. The cell consisted of an Al bottom plate (in contact with the back of the BDD) and a Teflon top piece, sandwiched together. A gasket was cut out of an ethylene propylene diene monomer (EPDM) sheet (McMaster-Carr, Cleveland, OH) to isolate the Al plate from contacting the electrolyte solution. A channel for the solution was cut into the Teflon piece and an inlet and outlet line was fed into/out of the cell using steel tubing, with the latter serving as the auxiliary electrode. A Luggin capillary for the non-aqueous Ag/AgCl electrode was constructed out of a glass pipette and a Pt wire was extended through the Teflon block to make electrical contact to the solution adjacent to the BDD electrode. The electrolysis solution was fed into the cell using a syringe pump so the reaction could be investigated on both flowing and stationary aliquots.

HPLC/PDA analysis

Reaction mixtures were analyzed on a Shimadzu 20LC with CBM 20A PDA detector. Separation (40 μL injection) was accomplished on a 25 cm × 4.6 mm, 5 μm C18 column using 60:40 water:methanol mobile phase at a flow rate of 2.5 mL/min with detection at 254 nm. The chromatograms showed three identifiable peaks attributed to **3** (rt 7.72 min; λ_{max} 206, 258, 305 nm), **1a** (rt 9.07 min; λ_{max} 200, 241, 288 nm) and **4** (rt 15.21 min; λ_{max} 200, 232, 289 nm).

REFERENCES

[1] P. W. Crawford, R. G. Scamehorn, U. Hollstein, M. D. Ryan, P. Kovacic, *Chem. Biol. Interact.* **1986**, *60*, 67.
[2] C. Olea-Azar, C. Rigol, F. Mendizabal, H. Cerecetto, M. R. Di, M. Gonzalez, W. Porcal, A. Morello, Y. Repetto, J. D. Maya, *Lett. Drug Des. Discov.* **2005**, *2*, 294.
[3] H. Cerecetto, M. R. Di, M. Gonzalez, M. Risso, P. Saenz, G. Seoane, A. Denicola, G. Peluffo, C. Quijano, C. Olea-Azar, *J. Med. Chem.* **1999**, *42*, 1941.
[4] K. Reybier, T. H. Y. Nguyen, H. Ibrahim, P. Perio, A. Montrose, P.-L. Fabre, F. Nepveu, *Bioelectrochemistry* **2012**, *88*, 57.
[5] I. Surov, H. Lund, *Acta Chem. Scand.* **1986**, *40*, 831.
[6] B. Soucaze-Guillous, H. Lund, *Acta Chem. Scand.* **1998**, *52*, 417.
[7] J.-M. Savéant, *Elements of Molecular and Biomolecular Electrochemistry: An Electrochemical Approach to Electron Transfer Chemistry*, Wiley-Interscience, Hoboken, NJ, **2006**.
[8] D. P. Valencia, F. J. Gonzalez, *Electrochem. Commun.* **2011**, *13*, 129.

Copyright © 2014 John Wiley & Sons, Ltd.

[9] J. Wang, G. M. Swain, M. Mermoux, G. Lucazeau, J. Zak, J. W. Strojek, *New Diamond Front. Carbon Technol.* **1999**, *9*, 317.
[10] A. J. Boulton, P. G. Tsoungas, *J. Chem. Soc. Perkin Trans.* **1986**, *1*, 1665.
[11] D. H. Evans, *Chem. Rev.* **1990**, *90*, 739.
[12] M. G. Kociolek, O. Hoermann, *Synthetic Comm.* **2012**, *42*, 2632.
[13] M. C. Granger, M. Witek, J. Xu, J. Wang, M. Hupert, A. Hanks, M. D. Koppang, J. E. Butler, G. Lucazeau, M. Mermoux, J. W. Strojek, G. M. Swain, *Anal. Chem.* **2000**, *72*, 3793.
[14] D. Y. Kim, J. C. Yang, H. W. Kim, G. M. Swain, *Electrochim. Acta* **2013**, *94*, 49.
[15] J. A. Bennett, G. M. Swain, *J. Electrochem. Soc.* **2010**, *157*, F89.

SUPPORTING INFORMATION

Additional supporting information may be found in the online version of this article at the publisher's website.

Copyright © 2014 John Wiley & Sons, Ltd.